



HAL
open science

The Components of Cepheid Systems: The FN Vel System

Nancy Ramage Evans, Pierre Kervella, Joanna Kuraszekiewicz, H. Moritz Günther, Richard I. Anderson, Charles Proffitt, Alexandre Gallenne, Antoine Mérand, Boris Trahin, Giordano Viviani, et al.

► **To cite this version:**

Nancy Ramage Evans, Pierre Kervella, Joanna Kuraszekiewicz, H. Moritz Günther, Richard I. Anderson, et al.. The Components of Cepheid Systems: The FN Vel System. *The Astronomical Journal*, 2024, 168, 10.3847/1538-3881/ad7fea . insu-04853403

HAL Id: insu-04853403

<https://insu.hal.science/insu-04853403v1>

Submitted on 24 Dec 2024

HAL is a multi-disciplinary open access archive for the deposit and dissemination of scientific research documents, whether they are published or not. The documents may come from teaching and research institutions in France or abroad, or from public or private research centers.

L'archive ouverte pluridisciplinaire **HAL**, est destinée au dépôt et à la diffusion de documents scientifiques de niveau recherche, publiés ou non, émanant des établissements d'enseignement et de recherche français ou étrangers, des laboratoires publics ou privés.



Distributed under a Creative Commons Attribution 4.0 International License



The Components of Cepheid Systems: The FN Vel System*

Nancy Ramage Evans¹ , Pierre Kervella² , Joanna Kurazskiewicz³ , H. Moritz Günther⁴ , Richard I. Anderson⁵ , Charles Proffitt⁶ , Alexandre Gallenne⁷ , Antoine Mérand⁸ , Boris Trahin², Giordano Viviani⁵, and Shreeya Shetye⁹

¹Smithsonian Astrophysical Observatory, MS 4, 60 Garden St., Cambridge, MA 02138, USA; nevans@cfa.harvard.edu

²LESIA, Observatoire de Paris, Université PSL, CNRS, Sorbonne Université, Université de Paris, 5 Place Jules Janssen, 92195 Meudon, France

³Smithsonian Astrophysical Observatory, MS 67, 60 Garden St., Cambridge, MA 02138, USA; jkurazskiewicz@cfa.harvard.edu

⁴Massachusetts Institute of Technology, Kavli Institute for Astrophysics and Space Research, 77 Massachusetts Ave., NE83-569, Cambridge, MA 02139, USA

⁵Institute of Physics, École Polytechnique Fédérale de Lausanne (EPFL), Observatoire de Sauverny, Chemin Pegasi 51B, 1290 Versoix, Switzerland

⁶Space Telescope Science Institute, 3700 San Martin Dr., Baltimore, MD 21218, USA

⁷Instituto de Astrofísica, Departamento de Ciencias Físicas, Facultad de Ciencias Exactas, Universidad Andrés Bello, Fernández Concha 700, Las Condes, Santiago, Chile and French-Chilean Laboratory for Astronomy, IRL 3386, CNRS, Casilla 36-D, Santiago, Chile

⁸European Southern Observatory, Karl-Schwarzschild-Str. 2, 85748 Garching, Germany

⁹Institute of Physics, École Polytechnique Fédérale de Lausanne (EPFL), Observatoire de Sauverny, Chemin Pegasi 51B, 1290 Versoix, Switzerland and Instituut voor Sterrenkunde, KU Leuven, Celestijnenlaan 200D bus 2401, Leuven, 3001, Belgium

Received 2024 July 11; revised 2024 September 17; accepted 2024 September 24; published 2024 October 24

Abstract

Cepheid masses continue to be important tests of evolutionary tracks for intermediate-mass stars as well as important predictors of their future fate. For systems where the secondary is a B star, Hubble Space Telescope ultraviolet spectra have been obtained. From these spectra a temperature can be derived, and from this a mass of the companion M_2 . Once Gaia DR4 is available, proper motions can be used to determine the inclination of the orbit. Combining mass of the companion, M_2 , the mass function from the ground-based orbit of the Cepheid and the inclination produces the mass of the Cepheid, M_1 . The Cepheid system FN Vel is used here to demonstrate this approach and what limits can be put on the Cepheid mass for inclination between 50° and 130° .

Unified Astronomy Thesaurus concepts: Cepheid variable stars (218); Stellar masses (1614)

1. Introduction

More than a century after the discovery of the Cepheid Leavitt (Period–Luminosity) Law, Cepheids continue to be the first step in the extragalactic distance scale (A. G. Riess et al. 2022; Breuval et al. 2024). This is of particular importance because of the tension between the Hubble constant from Cepheids and Type Ia supernovae and that from the early Universe based on Planck satellite cosmic microwave background observations (Riess et al. 2022). Cepheids are also a benchmark for calculations of evolutionary tracks, starting from their main-sequence progenitors (B stars). B stars are more plentiful than O stars and the calculations do not have to include large amounts of mass loss. Accurate modeling of evolutionary tracks to the Cepheid stage is an important step in predicting and modeling exotic end-stage objects resulting from a compact object in a multiple system (cataclysmic variables, some supernovae, and even gravitational waves). Cepheids will typically become white dwarfs but the more massive ones may ultimately become neutron stars. Massive and intermediate-mass stars are frequently found in binary or multiple systems (e.g., P. Kervella et al. 2019b). Specifically, Cepheids have a binary/multiple fraction of greater than $57\% \pm 12\%$ (N. R. Evans et al. 2022).

Ever since the first hydrodynamical pulsation calculations, it has been realized that masses predicted by evolutionary calculations are 10%–20% larger than those from pulsation calculations (see H. R. Neilson et al. 2011 for a summary). The difference has been somewhat reduced from investigations into opacities (e.g., Iglesias & Rogers 1996), core convective overshoot on the main sequence (e.g., P. G. Prada Moroni et al. 2012), pulsation-driven mass loss (H. R. Neilson et al. 2011), and rotation (R. I. Anderson et al. 2014). The effect of these parameters is complex. For example, while increased convective overshoot produces an appropriate luminosity, it limits the temperature increase of the blue loops where the Cepheids are found so that they do not enter the instability strip for many masses. It is likely that it is a combination of these that will reconcile the discrepancy.

Observational measurements of Cepheid masses are needed to test these predictions. Since there are no Cepheids in eclipsing binaries in the Milky Way (MW), there are two approaches available to measure masses. First, interferometry has created a group of resolved binaries, from which we can obtain the inclination i leading to both masses and distances (e.g., A. Gallenne et al. 2019). The first result is a mass of $4.29 \pm 0.13 M_\odot$ for the Cepheid V1334 Cyg (A. Gallenne et al. 2018), which uses velocities from the Hubble Space Telescope (HST) Space Telescope Imaging Spectrograph (STIS) high resolution spectra. It is significantly smaller than predictions of evolutionary tracks (N. R. Evans et al. 2018a). Second, satellite ultraviolet (UV) spectroscopy with HST has provided a group of double-lined spectroscopic binaries, for example, V350 Sgr (N. R. Evans et al. 2018b). Using the orbital velocity amplitude of the Cepheid (from the ground) and the amplitude of a hot companion (from the UV) and combining these two with a

* Based on observations with the NASA/ESA Hubble Space Telescope obtained at the Space Telescope Science Institute, which is operated by the Association of Universities for Research in Astronomy, Inc. under NASA contract NAS5-26555.



Original content from this work may be used under the terms of the [Creative Commons Attribution 4.0 licence](https://creativecommons.org/licenses/by/4.0/). Any further distribution of this work must maintain attribution to the author(s) and the title of the work, journal citation and DOI.

mass for the main-sequence companion inferred from the temperature provides the mass of the Cepheid.

A further motivation for determining the masses of MW Cepheids as accurately as possible is that six Cepheids (in five binary systems) have been found in eclipsing binaries in the Large Magellanic Cloud (LMC; B. Pilecki et al. 2018, 2021). This means comparison between the mass–luminosity relations for the metallicities of the MW and the LMC can now be made. Even this high-accuracy sample contains a warning. Of the five systems, two may have an evolutionary state different from the typical second or third crossing of the instability strip: first crossing and possible mass exchange systems.

This paper is a step toward an additional method to determine Cepheid masses. The mass function from a spectroscopic orbit combines the orbital period P and the foreshortened semimajor axis of the Cepheid ($A_1 \sin i$) into a function involving the masses of the Cepheid M and the companion m , and the inclination. For a reasonably massive companion (a B star), the companion dominates the spectrum in the far-ultraviolet (FUV). Furthermore, in this temperature range, the energy distribution is very sensitive to temperature. This means the temperature can be accurately determined, hence a mass can be inferred, which is the topic of this study.

FN Vel is a classical Cepheid with a pulsation period of 5.32^d and a mean V magnitude of 10.3 mag. It was discovered to be a spectroscopic binary by R. I. Anderson (2013) with an orbital period of 471.654^d and a velocity amplitude of 21.899 km s^{-1} . The Ca II H and K lines were discussed by V. Kovtyukh et al. (2015). From the relative strength of the H and K lines, they showed that the companion is a hot star.

For the FN Vel system, an orbit has recently been provided (S. Shetye et al. 2024). Proper motions from Gaia can add the inclination (P. Kervella et al. 2019b). However, for the FN Vel system, the orbital period of 1.29 yr is shorter than the observing windows for Hipparcos and Gaia DR3. This means the orbital velocity is smeared over the observing windows and is a lower limit to the true orbital velocity. It is not until the Gaia DR4 release when orbital motion will be included in the solutions that the inclination will be reliable and tightly constrained. At that time the combination of the mass function from the spectroscopic orbit, the mass of the companion, and the inclination from Gaia will provide the mass for the Cepheid itself.

This paper is a discussion of an HST STIS spectrum of the Cepheid FN Vel in the 1150–1700 Å region. It is the first in a project to obtain FUV spectra of the nine Cepheids with orbits (or at least orbital motion). For companions with B and A spectral types, temperatures and masses will be determined. For cooler companions, an upper limit to the temperature will result, which will add to the knowledge of the distribution of mass ratios in Cepheid systems. Masses will be derived from a study of masses of detached eclipsing binaries (DEBs) in the same spectral region (N. R. Evans et al. 2023).

The sections below discuss an HST STIS spectrum of the system, the energy distribution, temperature and mass of the companion, and the orbit and limits on the mass ratio and inclination of the system.

2. Observation

The FN Vel system was observed with the HST STIS Spectrograph on 2019 December 23 for 2480 s. The observation was with the G140L grating ($R \approx 1000$) with a wavelength range 1150–1700 Å in time-tag mode.

This program was designed to observe binary Cepheids where the companion had not yet been detected, and where the exact separation of the companion from the Cepheid was uncertain. We therefore took a number of steps to improve the faint detection limit. These included observing at the D1 aperture position in the 52X2 aperture, which puts the source below the region of the FUV MAMA detector, which can exhibit enhanced dark current, and observing in time-tag mode, which records the detection time of each photon. HST sees considerably reduced geocoronal background when in Earth’s shadow, and by using time-tag mode, we could potentially screen out the parts of the observation with the highest sky backgrounds. FN Vel turned out to be one of the brighter Cepheid companions found in this program, and so for this target, these extra precautions were not needed.

Data processing was done with the standard HST CALSTIS pipeline as described in S. T. Sohn (2019). As part of the extraction process for point sources, CALSTIS does a cross-correlation of the 2D flat-fielded spectral image using the expected shape of the spectral trace on the detector to centroid the spectrum and locate the extraction region to be used. Line lamp exposures are also taken to measure flexure in the STIS optical bench in both the dispersion and cross-dispersion direction. Since the narrow band F28X50OIII filter with an effective wavelength of about 5008 Å was used for the target acquisition, it was the Cepheid itself rather than the hot companion that was placed at the 52X2D1 aperture location. However, comparing the results of the cross-correlation of the FUV spectrum with the expected spectral location as determined using the lamp images shows an offset of only about 3 mas, which is small compared to the expected uncertainty in the target acquisition. Thus, the STIS data finds no significant offset between the Cepheid FN Vel and its hot companion, although this measure is only sensitive to offsets in the cross-dispersion direction, which in this case corresponds to a position angle of $266^\circ.15$ east of north.

3. Energy Distribution

3.1. $E(B - V)$

The reddening of the FN Vel system is significant, and important in interpreting the STIS spectrum. The star is faint enough that it has not been as intensively studied as brighter Cepheids. F. Van Leeuwen et al. (2007) summarize the integrated mean photometry for the system $\langle B \rangle$, $\langle V \rangle$, and $\langle I_C \rangle$. They list a reddening $E(B - V)$ of 0.558 mag. The photometry can also be used to calculate $E(B - V)$ on the system of J. F. Dean et al. (1978), using the relation from J. D. Fernie (1990). This is useful since we know the photometry contains contributions from both the Cepheid and the hot companion. Here we explore whether the contribution from the companion affects the derived reddening significantly.

Anticipating the result below, the spectrum from 1100 to 1700 Å is well matched by an atmosphere with a temperature of 15000 K from the BOSZ Kurucz Atlas9 atmospheres (R. C. Bohlin et al. 2017). Using the calibration of M. J. Pecaut & E. E. Mamajek (2013), this is midway between B5 and B6 main sequence stars, which we will call B5.5 with $B - V = -0.148$ mag and $(V - I)_C = -0.155$ mag. The calibration of Drilling & Landolt (2000; Table 15.7) provides M_V of -1.1 mag for a B5.5 V star. The absolute magnitude of the Cepheid M_V is -3.68 mag from Cruz Reyes & Anderson (2023;

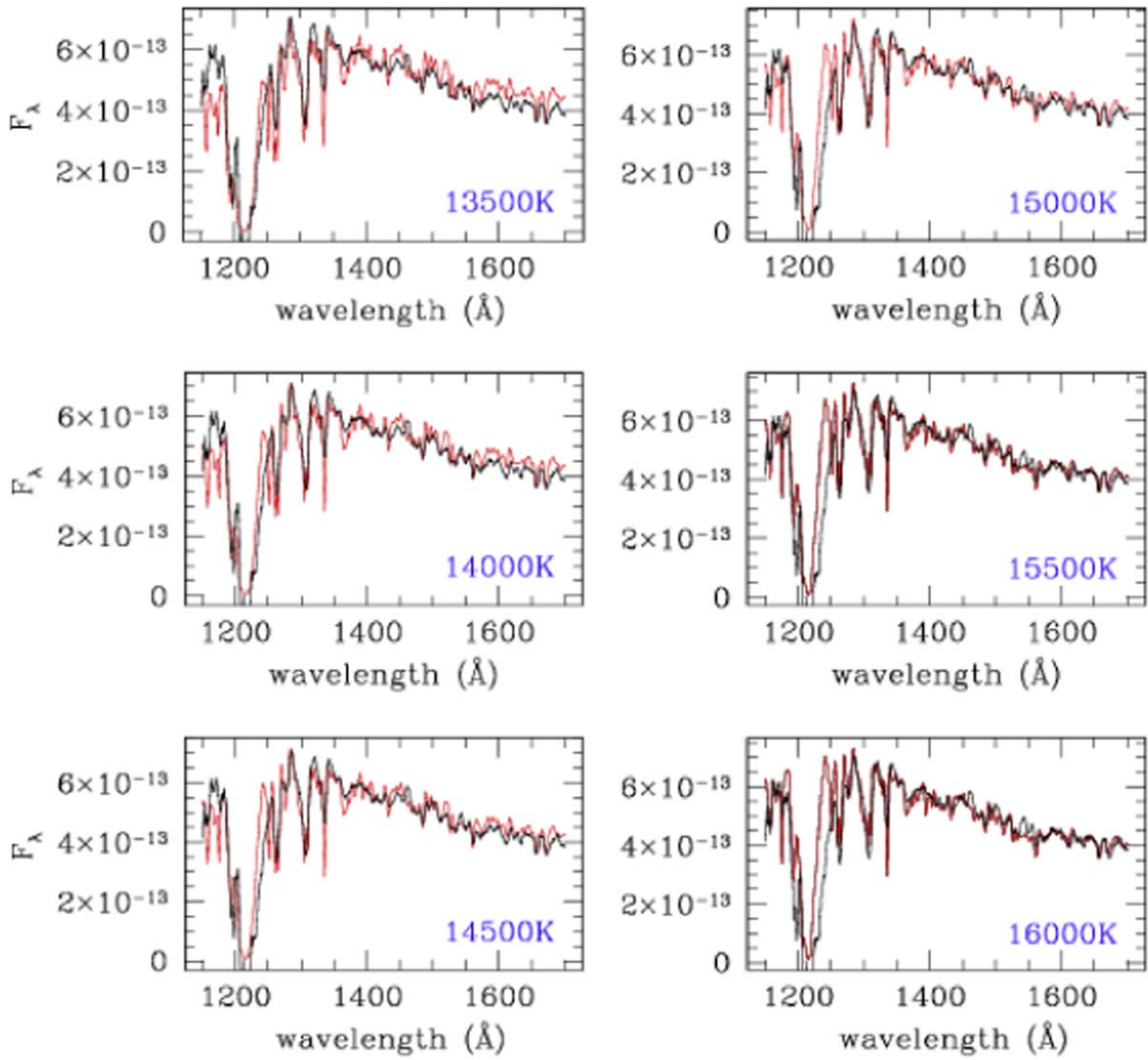


Figure 1. Comparison between BOSZ models and the STIS spectrum unreddened for $E(B - V) = 0.60$ mag. Flux for all panels is in $\text{erg cm}^{-2} \text{s}^{-1} \text{\AA}^{-1}$; wavelength is in \AA . Models are in red; spectrum is in black. The temperature for the models is at the lower right of each panel.

Table 1
Correction for Companion

	$\langle B \rangle$	$\langle V \rangle$	$\langle I \rangle$
Cepheid + Companion	11.48	10.29	8.83
Cepheid	11.68	10.39	8.88
Companion	13.42	12.97	12.34

Table 1) from Gaia DR3 data for Cepheids and open clusters. Using the magnitude difference between the Cepheid and the B5.5 V star the correction to $\langle B \rangle$, $\langle V \rangle$, and $\langle I_C \rangle$ were computed in Table 1.

From these, the original $\langle B \rangle - \langle V \rangle$ and $\langle V \rangle - \langle I_C \rangle$ of 1.185 and 1.461 mag become 1.27 and 1.50 mag. Using the appropriate reddening formula from J. D. Fernie (1990), $E(B - V)$ is 0.59 mag (Table 2). That is, it is little affected by the companion.

4. Companion Temperature

The temperature of the companion FN Vel B was determined by comparison of the spectrum with BOSZ model atmospheres

Table 2
Reddening

	$\langle B \rangle - \langle V \rangle$ (mag)	$\langle V \rangle - \langle I \rangle$ (mag)	$E(B - V)$ (mag)
Corrected	1.27	1.50	0.59
Original	1.19	1.46	0.61
van Leeuwen	0.558

computed from Kurucz Atlas9 code (R. C. Bohlin et al. 2017). The details of the approach are presented in N. R. Evans et al. (2023). The spectrum is compared with atmospheres through a series of temperatures in steps of 500 K. The BOSZ models selected have solar abundance, surface gravity ($\log g$) of 4.0, microturbulence of 2 km s^{-1} , and instrumental broadening of 500 km s^{-1} , selected to match the STIS spectrum of a main-sequence star.

Recently a revised version of the BOSZ models has been made available (S. Meszaros et al. 2024). The revisions include using both MARCS and Atlas9 atmospheres, as well as updated opacities. We have investigated the differences the

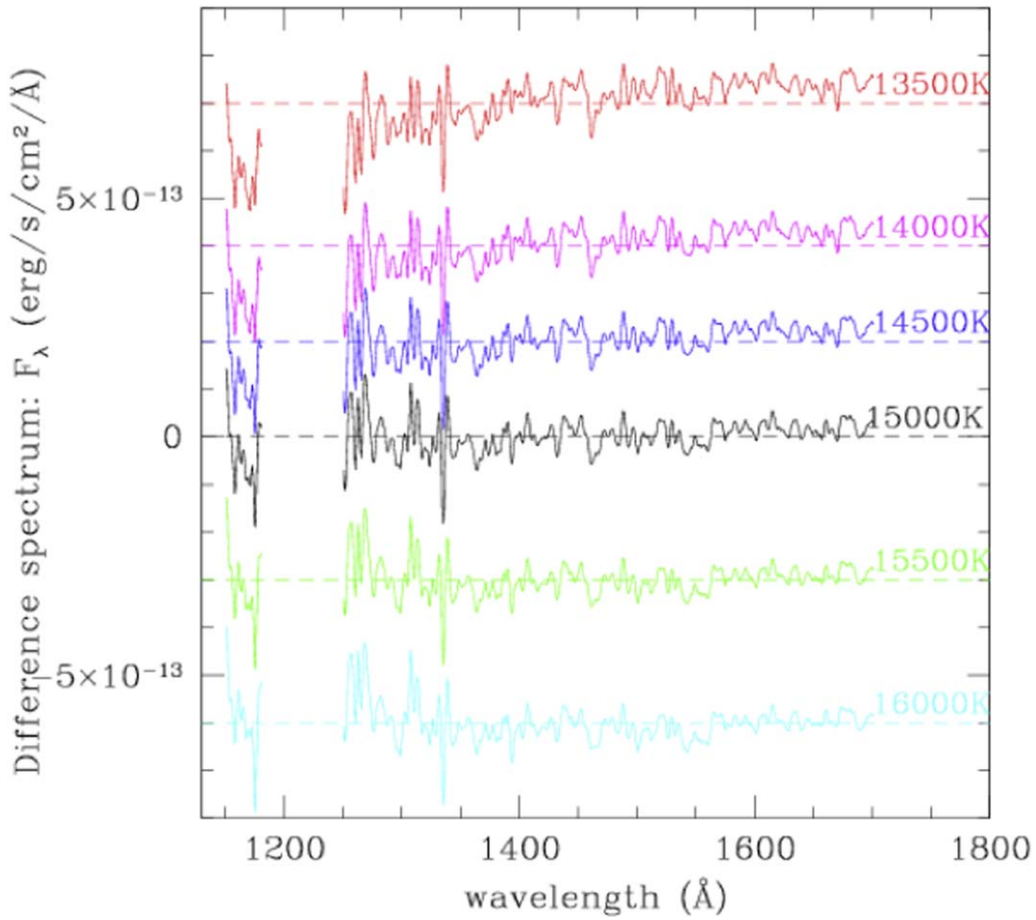


Figure 2. The difference between the model and the spectrum for $E(B - V) = 0.60$ mag. The temperatures for the models are on the right of each difference spectrum. The wavelengths between 1180 and 1250 Å are omitted because of contamination by interstellar Ly α absorption. The difference spectrum in black is the best fit.

new models make. Because of the increased opacity in the UV, the solutions are driven to higher temperatures. The MK spectral B5 V standard ρ Aur was also found to be hotter than the Pecaut and Mamajek temperature for B5 V of 15,700 K. Although the 1150–1270 Å region is clearly sensitive to temperature, the temperatures derived from the models themselves have some uncertainty. However, in this study of the companion to the Cepheid FN Vel, we use the temperature only to identify DEB spectra of the same temperature (from the same 2017 models) and deduce the mass from the comparison. Thus, the resulting mass for FN Vel B should be accurate, and we will continue to use the 2017 BOSZ models.

As discussed in N. R. Evans et al. (2024), there are a number of strong features of Si II and C II between 1250 and 1350 Å, which are temperature sensitive. However, we do not attempt to model them directly in the low-resolution spectrum.

Figure 1 shows the spectrum (black) compared with models for a series of temperatures. Figure 2 shows the spectrum differences for these temperatures. The Ly α region from 1180 to 1250 Å is omitted in the fit, because of contamination from interstellar Ly α . The progression of the difference spectra from 13,500 to 16,000 K illustrates the deficit of flux at the shortest wavelengths in the models for the coolest models. The hotter models have increased flux relative to the companion at the shortest wavelengths.

The determination of the best-fit temperature is shown in Figure 3 from the standard deviation of the difference spectra as a function of temperature. The parabola fits are shown for two reddenings, $E(B - V) = 0.60$ and 0.56 mag. Table 3 lists the

Table 3
FN Vel B Temperature

$E(B - V)$	T (K)	Err SD (K)	Err Vis (K)
0.56	14,535	360	500
0.60	15,391	629	500

temperatures for these reddenings. The errors are the error from the parabola fit (Err SD), and the errors from the visual comparison of the difference spectra (Err Vis), as discussed in N. R. Evans et al. (2023). The difference in temperature for the two reddenings is within the errors, confirming that the temperature determinations are not dominated by uncertainty in reddening. Table 3 shows that although the spectra are from the UV wavelength region, the energy distribution is not highly sensitive to the reddening. This is because the spectrum only covers 600 Å, and its shape is very sensitive to temperature, particularly around Ly α .

5. Companion Mass

The relation between mass and temperature was determined for DEBs with B and early A dwarfs (N. R. Evans et al. 2023). In this study, International Ultraviolet Explorer satellite spectra of DEBs in the same wavelength region as the STIS spectrum of FN Vel were compared with a series of BOSZ models to determine the temperature of the primary. These temperatures were combined with the masses of the DEBs

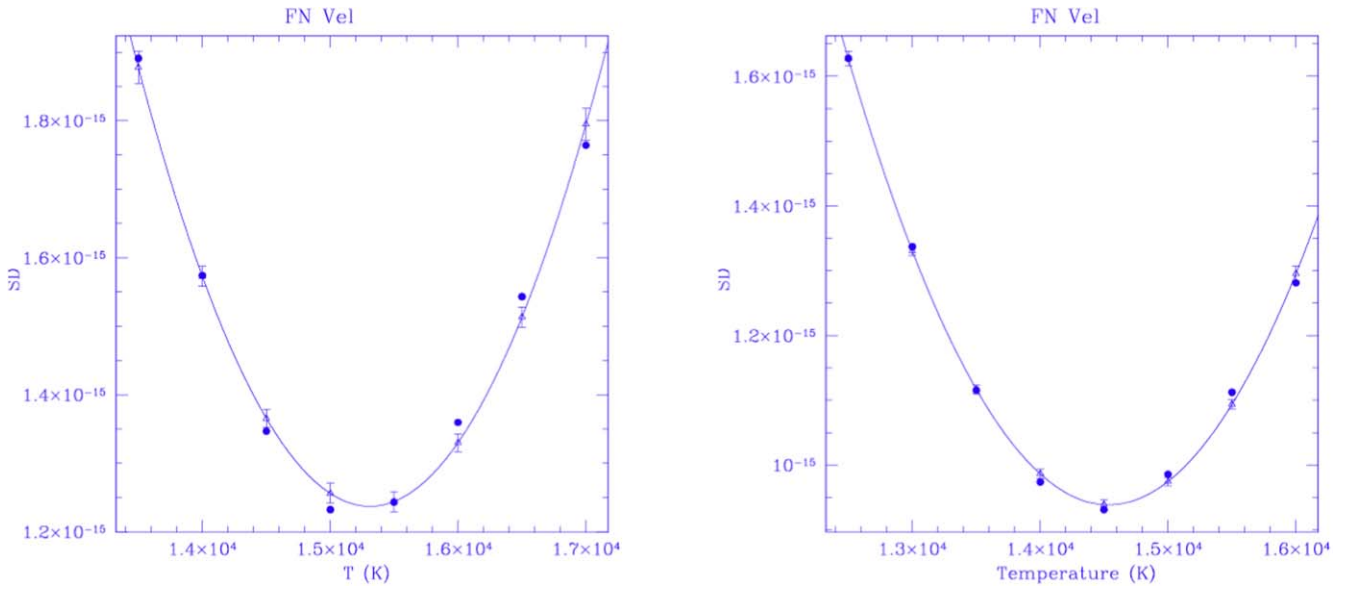


Figure 3. The standard deviations from the spectrum-model comparison as the temperature of the models is changed. Dots: the standard deviation; triangles: the parabola fit. Left: $E(B - V) = 0.60$ mag. Right: $E(B - V) = 0.56$ mag.

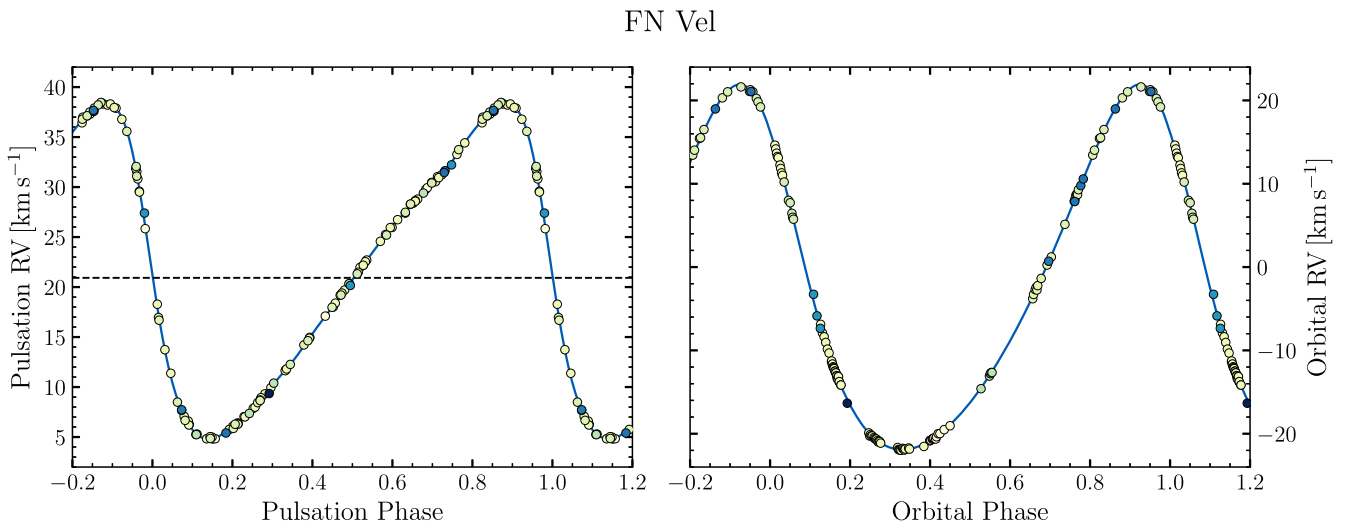


Figure 4. The pulsation velocity (left) and the orbital velocity (right) are shown as a function of their respective phases. The dashed line in the left figure is the systemic velocity. The colors of the symbols indicate the date of observation from the earliest data in yellow to more recent data in blue. (Adapted from S. Shetye et al. 2024).

from G. Torres et al. (2010) to derive the mass–temperature relation. The rms of the residuals from this relation is 0.037 in $\log M$. Rotation and abundance difference contribute to the spread in this relation, as does age spread within the main sequence. An estimate of the time on the main sequence (S. Ekström et al. 2012) results in ± 0.04 in $\log M$. That is, the duration of the main-sequence life could account for the entire spread. The companions of Cepheids are a special case within main-sequence stars since they are the companions of more massive stars, and hence belong to the younger part of the DEB sample. For this reason, we use a mass–temperature relation to interpret Cepheids, which is 0.02 smaller in $\log M$ than that for DEBs.

Table 4 illustrates the sensitivity of the mass of FN Vel B to the temperature from the STIS spectrum for a plausible range of temperatures.

Table 4
Mass of FN Vel B

Temperature (K)	Mass (M_{\odot})
14,900	3.89
15,400	4.09
15,900	4.31

6. Orbit

Further progress in obtaining the masses of both the Cepheid and the companion in the FN Vel system makes use of a spectroscopic orbit.

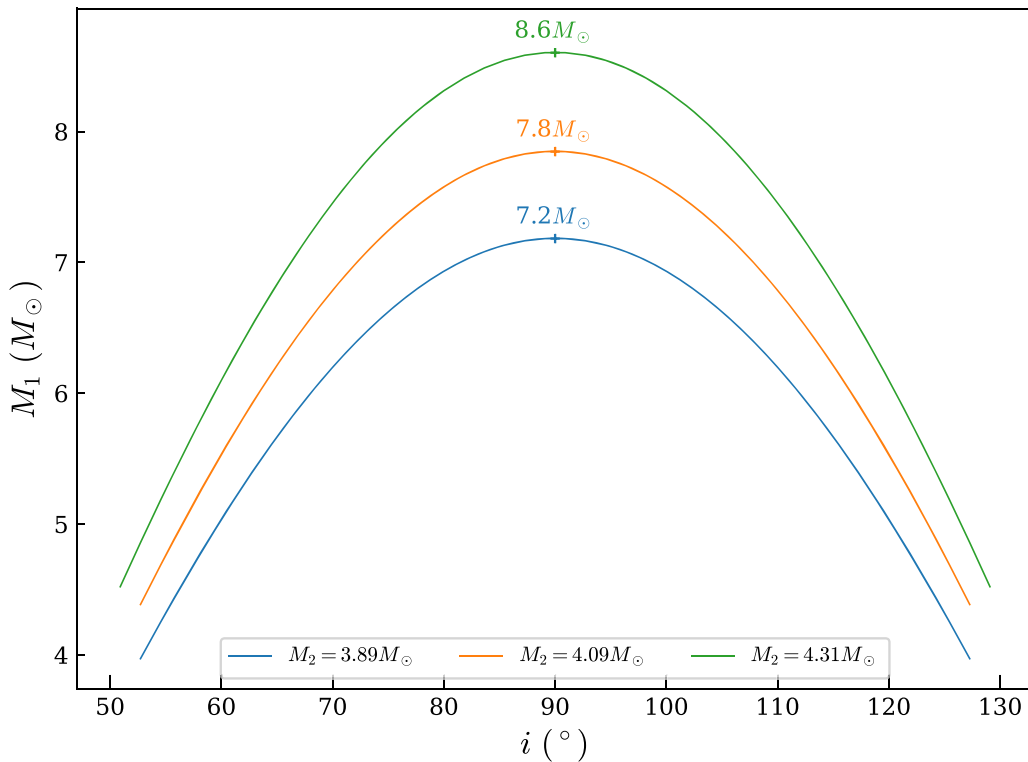


Figure 5. The Cepheid mass as a function of inclination and the mass of the companion. The lines show the relation for the range of companion masses M_2 in Table 4: $3.89 M_\odot$: blue; $4.09 M_\odot$: red; $4.31 M_\odot$: green. The maximum value of the Cepheid mass M_1 is listed above the curves for the companion masses M_2 .

Table 5
FN Vel Orbit

Parameters	Units	
P_{orb}	(yr)	1.2917 ± 0.0002
T_0	(JD)	$2,456,407.87 \pm 0.36$
e	...	0.218 ± 0.001
K	(km s^{-1})	21.91 ± 0.02
ω	($^\circ$)	42.07 ± 0.21
$A_1 \sin i$	(au)	0.927 ± 0.001
$f(m)$	(M_\odot)	0.48 ± 0.0017

6.1. Spectroscopic Orbit

We discuss here briefly the spectroscopic orbit of the FN Vel system. New radial velocities for the FN Vel binary since its discovery have been obtained (R. I. Anderson et al. 2024) in the VELOCE program. An orbit has been determined in S. Shetye et al. (2024). The results are shown in Figure 4 adapted from Shetye et al. The parameters from the orbit are in Table 5.

The spectroscopic orbit provides the mass function:

$$F(M, m) = m^3 \sin^3 i / (M + m)^2 = (A_1 \sin i)^3 / P^2,$$

where M and m are the masses of the Cepheid and the companion, respectively, in solar masses, P is the orbital period in years, and $(A_1 \sin i)$ is the foreshortened semimajor axis of the Cepheid in astronomical units.

The remaining parameter needed to determine the Cepheid mass is the inclination. Ultimately, this will be provided by Gaia. Proper motions from Gaia and those from Hipparcos (and a distance) combined with a spectroscopic orbit provide complete velocity data for the orbit, and hence an inclination

as discussed by P. Kervella et al. (2019b). As pointed out there, the proper motions from those two catalogs are not instantaneous, but an average over the observing window. For Cepheids with orbital periods shorter than those observing windows (as is the case for FN Vel), the smearing results in a decreased proper motion. The smearing can be imperfectly approximated (P. Kervella et al. 2019a) for the ratio of the orbital period to the Gaia DR3 observing window (472/1038). Unfortunately, this estimate produces an inclination too uncertain to provide usable results. This will be revisited when the Gaia DR4 release includes astrometric orbital fitting. Furthermore, the longer observation stream in the Gaia DR4 release will remove the dependency on the relatively large Hipparcos uncertainty.

7. Discussion and Conclusions

In summary, in the FN Vel binary system, the mass of the companion has been determined from the energy distribution from an STIS UV spectrum. An orbit is now available. The remaining parameter required to determine the mass of the system is the inclination of the orbit. This will be available from the Gaia DR4 data release.

With the available data, some limits can be placed on the Cepheid mass. Using the mass function from Table 5 with the companion mass from Table 4, the Cepheid mass can be calculated for values of the inclination. Figure 5 shows that for the inclination between 50° and 130° , the Cepheid mass is between 4 and $9 M_\odot$.

To connect the Cepheid FN Vel with its past history, the Achernar system appears to be a good model for a progenitor (P. Kervella et al. 2022). It is a Be star (A) with an A star companion (B). The mass for A has recently been determined

to be $6.0 \pm 0.6 M_{\odot}$ with an orbital period of 7 yr. The separation between A and B is large enough that it is anticipated that A will evolve to become a Cepheid without mass exchange between the components. Because the orbital period of FN Vel is shorter, the question is raised whether mass exchange within the system has occurred in the past, particularly when the primary was at the tip of the red giant branch. Systems such as FN Vel are a good probe of this question. One indication of past history is the summary of orbit parameters for Cepheids (S. Shetye et al. 2024). The orbital period of FN Vel is just on the boundary of periods where Cepheid systems exist. With a pulsation period of 5 days, it is not an unusually large Cepheid. Furthermore, the system has not been fully circularized. Thus, the system seems to have at most had mild mass exchange. However, as an additional system very close to the limit of mass exchange it is a useful data point.









To summarize, after the Gaia DR4 release, the combination of a mass for the secondary FN Vel B, a spectroscopic orbit, and an inclination will provide a mass for the Cepheid, FN Vel A. This is valuable for comparison with evolutionary calculations.

Acknowledgments

Support for J.K. and C.P. was provided from HST-GO-15861.001-A. Support was provided to N.R.E. by the Chandra X-ray Center NASA Contract NAS8-03060. H.M.G. was supported through grant HST-GO-15861.005-A from the STScI under NASA contract NAS5-26555. This project has received funding from the European Research Council (ERC) under the European Union’s Horizon 2020 research and innovation program to P.K. (projects CepBin, grant agreement No. 695099, and UniverScale, grant agreement No. 951549). RIA is funded by the SNSF through an Eccellenza Professorial Fellowship, grant No. PCEFP2_194638. This project has received funding from the European Research Council (ERC) under the European Union’s Horizon 2020 research and innovation program (grant Agreement No. 947660). S.S. would like to acknowledge the Research Foundation-Flanders (grant No. 1239522N). A.G. acknowledges the support of the Agencia Nacional de Investigación Científica y Desarrollo (ANID) through the FONDECYT Regular grant 1241073. This work has made use of data from the European Space Agency (ESA) mission Gaia (<https://www.cosmos.esa.int/gaia>), processed by the Gaia Data Processing and Analysis Consortium (DPAC, <https://www.cosmos.esa.int/web/gaia/dpac/consortium>). Funding for the DPAC has been provided by national institutions, in particular, the institutions participating in the Gaia Multilateral Agreement. The SIMBAD database and NASA’s Astrophysics Data System Bibliographic Services were used in the preparation of this paper.

The data presented in this article were obtained from the Mikulski Archive for Space Telescopes (MAST) at the Space Telescope Science Institute. The specific observations analyzed can be accessed via doi:[10.17909/m493-xr06](https://doi.org/10.17909/m493-xr06).

ORCID iDs

Nancy Remage Evans  <https://orcid.org/0000-0002-4374-075X>
 Pierre Kervella  <https://orcid.org/0000-0003-0626-1749>
 Joanna Kuraszkiwicz  <https://orcid.org/0000-0001-5513-029X>
 H. Moritz Günther  <https://orcid.org/0000-0003-4243-2840>
 Richard I. Anderson  <https://orcid.org/0000-0001-8089-4419>
 Charles Proffitt  <https://orcid.org/0000-0001-7617-5665>
 Alexandre Gallenne  <https://orcid.org/0000-0001-7853-4094>
 Antoine Mérand  <https://orcid.org/0000-0003-2125-0183>

References

- Anderson, R. I. 2013, PhD Thesis, Univ. of Geneva
 Anderson, R. I., Ekström, S., Georgy, C., et al. 2014, *A&A*, 564, A100
 Anderson, R. I., Viviani, G., Shetye, S., et al. 2024, *A&A*, 686, A177
 Bohlin, R. C., Meszaros, S., Fleming, S. W., et al. 2017, *AJ*, 153, 234
 Breuval, L., Riess, A. G., Casertano, S., et al. 2024, *ApJ*, 973, 30
 Cruz Reyes, M., & Anderson, R. I. 2023, *A&A*, 672, A85
 Dean, J. F., Warren, P. R., & Cousins, A. W. J. 1978, *MNRAS*, 183, 569
 Drilling, J. S., & Landolt, A. U. 2000, in *Astrophysical Quantities*, ed. A. N. Cox (New York: Springer)
 Ekström, S., Georgy, C., Eggenberger, P., et al. 2012, *A&A*, 537, A146
 Evans, N. R., Engle, S., Pillitteri, I., et al. 2022, *ApJ*, 938, 153
 Evans, N. R., Ferrari, M. G., Kuraszkiwicz, J., et al. 2023, *AJ*, 166, 109
 Evans, N. R., Gallenne, A., Kervella, P., et al. 2024, *ApJ*, 972, 145
 Evans, N. R., Karovska, M., Bond, H. E., et al. 2018a, *ApJ*, 863, 187
 Evans, N. R., Proffitt, C., Carpenter, K. G., et al. 2018b, *ApJ*, 866, 30
 Fernie, J. D. 1990, *ApJS*, 72, 153
 Gallenne, A., Kervella, P., Borgniet, S., et al. 2019, *A&A*, 622, 164
 Gallenne, A., Kervella, P., Evans, N. R., et al. 2018, *ApJ*, 867, 121
 Iglesias, C. A., & Rogers, F. J. 1996, *ApJ*, 464, 943
 Kervella, P., Arenou, F., Mignard, F., & Thévenin, F. 2019a, *A&A*, 623, A72
 Kervella, P., Borgniet, S., Domiciano de Souza, A., et al. 2022, *A&A*, 667, A111
 Kervella, P., Gallenne, A., Evans, N. R., et al. 2019b, *A&A*, 623, A116
 Kovtyukh, V., Szabados, L., Chekhonadskikh, F., Lemasle, B., & Belik, S. 2015, *MNRAS*, 448, 3567
 Meszaros, S., Bohlin, R., Prieto, C. A., et al. 2024, *A&A*, 688, 197
 Neilson, H. R., Cantiello, M., & Langer, N. 2011, *A&A*, 529, L9
 Pecaut, M. J., & Mamajek, E. E. 2013, *ApJS*, 208, 9
 Pilecki, B., Gieren, W., Pietrzynski, G., et al. 2018, *ApJ*, 862, 43
 Pilecki, B., Pietrzynski, G., Anderson, R. I., et al. 2021, *ApJ*, 910, 118
 Prada Moroni, P. G., Gennaro, M., Bono, G., et al. 2012, *ApJ*, 749, 108
 Riess, A. G., Yuan, W., Macri, L. M., et al. 2022, *ApJ*, 934, L7
 Shetye, S., Anderson, R. I., Viviani, G., et al. 2024, arXiv:2405.19840
 Sohn, S. T., Branton, D., Carlberg, J., et al. 2019, “STIS Data Handbook” Version 7.0 (Baltimore, MD: STScI)
 Torres, G., Andersen, J., & Gimenez, A. 2010, *A&ARv*, 18, 67
 Van Leeuwen, F., Feast, M. W., Whitelock, P. A., & Laney, C. D. 2007, *MNRAS*, 379, 723